

# A THEORETICAL STUDY OF A SIMPLIFIED AIR-SEA COUPLING PROBLEM INCLUDING TURBULENT PARAMETERIZATIONS

C. PELLETIER\*, F. LEMARIÉ<sup>†</sup> AND E. BLAYO\*

<sup>†</sup>Corresponding author : Inria, Univ. Grenoble-Alpes, CNRS, LJK  
F-38000, Grenoble, France  
e-mail: [florian.lemarie@inria.fr](mailto:florian.lemarie@inria.fr) - Web page: <https://team.inria.fr/airsea/en/>

\* Univ. Grenoble-Alpes, CNRS, LJK, Inria  
F-38000, Grenoble, France  
e-mail: [charles.pelletier@univ-grenoble-alpes.fr](mailto:charles.pelletier@univ-grenoble-alpes.fr), [eric.blayo@univ-grenoble-alpes.fr](mailto:eric.blayo@univ-grenoble-alpes.fr)

**Key words:** Multiphysics coupling, Air-sea interface, Subgrid scales parameterizations, Ekman boundary layers

**Abstract.** In this paper we study a simplified mathematical model representative of air-sea coupling. This model incorporates parameterizations of the turbulent boundary layers as used in realistic models. We show that even if simple equations like the one-dimensional stationary heat equation are considered the presence of parameterizations renders the problem extremely complex to study and the unicity of solutions is no longer guaranteed. We motivate and describe a coupling algorithm which ensures that a unique physically sound solution is obtained.

## 1 INTRODUCTION

The use of fully coupled ocean-atmosphere models has become widespread in recent years. Historically limited to global climate studies, such models are now routinely used for regional and coastal applications. There is yet no systematic studies carefully investigating the formulation of atmospheric and oceanic coupled models including the interplay between numerical and physical aspects. Proper representation of air-sea interactions in such models cover a large range of issues: parameterization of atmospheric and oceanic boundary layers, estimation of air-sea fluxes, time-space numerical schemes, non conforming grids, coupling algorithms... Several coupling methods, whose precise contents, theoretical justification and stability properties are often somewhat difficult to compare precisely, are presently used in actual applications [1, 2]. In this context, our objective is to study more systematically the numerical properties of coupling algorithms used for practical applications to clarify their merits and flaws and establish more robust methods.

The oceanic and atmospheric models must rely on parameterization schemes to account for unresolved scales. Those parameterizations are essential to maintain a reasonable level of plausibility of the numerical solutions, but their mathematical formulation is often devised empirically and can impair the regularity of the associated solutions (e.g. [3]). Moreover, sub-grid scales parameterization schemes used for representing the oceanic and atmospheric boundary layers and for computing the turbulent components of air-sea fluxes are generally developed independently, without any guarantee regarding the well-posedness of the overall coupled problem. This latter aspect will be specifically addressed in this paper using a simplified mathematical model representative of most of the delicacies arising in air-sea coupling problems. We propose to analyze the so-called coupled Ekman boundary layer problem. Several aspects of this problem have already been studied in [4, 5]. In the present study we extend these works by incorporating parameterizations of the turbulent boundary layers as used in realistic models.

The paper is organized as follows. Section 2 motivates and introduces the coupled problem under interest. Theoretical mathematical results are presented in Section 3 to emphasize how the parameterization schemes could alter the well-posedness of the coupled problem. Finally, Section 4 describes a consistent coupling algorithm and numerical results are shown to illustrate some of the aspects previously discussed.

## 2 THE MATHEMATICAL MODEL

Most state-of-the-art atmospheric and oceanic models solve the stratified Reynolds-averaged Navier-Stokes equations (in the following we will note  $\langle \cdot \rangle$  the Reynolds averaging operator) with possibly additional simplifying assumptions like the hydrostatic, Boussinesq or so-called traditional assumptions. Due to the complexity of those equations, it is customary to work with simplified equations sets to focus on specific problems. In particular, studies of turbulent mixing traditionally rely on the horizontal homogeneity assumption (i.e.  $\partial_x = \partial_y = 0$ ) and neglect vertical advection which is considered a small effect compared to vertical mixing in the vicinity of the air-sea interface [6, 7]. For this preliminary study, we also assume the absence of stratification (i.e. potential temperature, seawater salinity and air humidity are held constant).

### 2.1 The coupled Ekman layer problem

We define two subdomains  $\Omega_a = ]z_a^1; z_a^\infty[$  and  $\Omega_o = ]z_o^\infty; z_o^1[$  with  $0 < z_a^1 < z_a^\infty$  and  $z_o^\infty < z_o^1 < 0$  as well as a time interval  $[0, T]$ . Under the various assumptions presented so far, the problem of interest reads, for a given initial condition,

$$\left\{ \begin{array}{ll} \partial_t \mathbf{u}_a - f \mathbf{k} \times (\mathbf{u}_a - \mathbf{u}_a^g) + \partial_z \langle w'_a \mathbf{u}'_a \rangle &= 0, & \text{in } \Omega_a \times [0, T] \\ \mathbf{u}_a(z = z_a^\infty, t) &= \mathbf{u}_a^g, & \text{in } [0, T] \\ \rho_a \langle w'_a \mathbf{u}'_a \rangle(z = z_a^1, t) &= \rho_o \langle w'_o \mathbf{u}'_o \rangle(z = z_o^1, t), & \text{in } [0, T] \end{array} \right. \quad (2.1)$$

$$\left\{ \begin{array}{ll} \partial_t \mathbf{u}_o - f \mathbf{k} \times (\mathbf{u}_o - \mathbf{u}_o^g) + \partial_z \langle w'_o \mathbf{u}'_o \rangle &= 0, & \text{in } \Omega_o \times [0, T] \\ \mathbf{u}_o(z = z_o^\infty, t) &= \mathbf{u}_o^g, & \text{in } [0, T] \\ \rho_o \langle w'_o \mathbf{u}'_o \rangle(z = z_o^1, t) &= \rho_a \langle w'_a \mathbf{u}'_a \rangle(z = z_a^1, t), & \text{in } [0, T] \end{array} \right. \quad (2.2)$$

where  $\mathbf{u}_\alpha = (u_{\alpha,x}, u_{\alpha,y})$ , ( $\alpha = o, a$ ) is the horizontal velocity vector in the fluid of density  $\rho_\alpha$ ,  $\mathbf{u}_\alpha^g$  corresponds to a prescribed large-scale geostrophic forcing,  $w'_\alpha$  is the vertical velocity fluctuation,  $f$  represents the Coriolis frequency associated to earth rotation and  $\mathbf{k}$  is a unit vector in the vertical direction. In (2.1) and (2.2) the terms in the form  $\langle w'_\alpha \mathbf{u}'_\alpha \rangle$  are the vertical components of the Reynolds stress tensor associated to turbulent sub-grid scales fluctuations. Coupled problem (2.1-2.2) corresponds to the so-called Ekman equations which are for instance often used to study the wind-driven motions in the ocean. To fully define the problem under investigation, additional closure assumptions need to be made to express the  $\langle w'_\alpha \mathbf{u}'_\alpha \rangle$  terms.

## 2.2 Closure assumptions

This section introduces parameterizations to express  $\langle w'_a \mathbf{u}'_a \rangle(z, t)$  in the atmospheric boundary layer,  $\langle w'_o \mathbf{u}'_o \rangle(z, t)$  in the oceanic boundary layer and  $\langle w'_\alpha \mathbf{u}'_\alpha \rangle$  in the surface layer (i.e. in  $\Omega_\Gamma = ]z_o^1, z_a^1[$ ).

### 2.2.1 Surface layer parameterization

In the absence of stratification the turbulent flow in the vicinity of the air-sea interface is given by a classical law of the wall which stipulates that the velocity is proportional to the logarithm of the distance from the interface :

$$\mathbf{u}_a(z) = \mathbf{u}_a(z_a^r) + \frac{u_a^*}{\kappa} \ln(z/z_a^r) \mathbf{e}_\tau, \quad \text{for } z \in ]z_a^r, z_a^1[ \quad (2.3)$$

$$\mathbf{u}_o(z) = \mathbf{u}_o(z_o^r) - \frac{u_o^*}{\kappa} \ln(z/z_o^r) \mathbf{e}_\tau, \quad \text{for } z \in ]z_o^1, z_o^r[ \quad (2.4)$$

with  $u_\alpha^*$  a friction velocity,  $\kappa$  the von Karman constant,  $z_{r,\alpha}$  the roughness lengths to be defined delimiting a viscous sublayer, and  $\mathbf{e}_\tau$  a unit vector in the direction of  $[\![\mathbf{u}]\!]_0^{z_a^1} = \mathbf{u}_a(z_a^1) - \mathbf{u}_a(0) (= \mathbf{u}_a(z_a^1) - \mathbf{u}_o(0))$ . The Reynolds stress component in the surface layer is given by

$$\langle w'_\alpha \mathbf{u}'_\alpha \rangle = -(u_\alpha^*)^2 \mathbf{e}_\tau$$

where  $u_\alpha^*$  is computed thanks to (2.3) and (2.4) using atmospheric and oceanic inputs at  $z = z_a^1$  and  $z = z_o^1$ . The roughness lengths are

$$z_a^r(u_a^*) = a \frac{u_a^{*2}}{g} + b \frac{\nu_a}{u_a^*}, \quad z_o^r = -\frac{u_o^*}{u_a^*} z_a^r \quad (2.5)$$

which is derived from [8], where  $a$ ,  $b$ ,  $g$  and  $\nu_a$  are all known constants. The condition on  $z_o^r$  ensures the  $\mathcal{C}^1$  character of the solution profiles at the crossing of the interface  $z = 0$ , assuming the wind stress  $\boldsymbol{\tau} = \rho_a (u_a^*)^2 \mathbf{e}_\tau$  is constant in the surface layer, and that the solution has constant vertical gradient in  $]z_o^r, z_a^r[$ .

### 2.2.2 Boundary layer parameterization

Considering that turbulence acts as mixing, the usual closure assumption used in the overwhelming majority of numerical models is

$$\langle w'_\alpha \mathbf{u}'_\alpha \rangle(z) = -\nu_\alpha \partial_z \mathbf{u}_\alpha$$

where  $\nu_\alpha$  is a flow-dependent turbulent viscosity. In the absence of stratification, a typical way of computing  $\nu_\alpha$ , based on the so-called K-profile parameterization (KPP), is given in [7] :

$$\nu_\alpha(u_\alpha^*, z) = \frac{c\kappa u_\alpha^{*2}}{|f|} G(\sigma) H(1 - \sigma) + \nu_\alpha^m \quad \text{where} \quad \begin{cases} c := 0.7, \kappa := 0.41, \sigma := \frac{|z|}{h_{pbl}^\alpha(u_\alpha^*)} \\ h_{pbl}^\alpha(u_\alpha^*) := \frac{cu_\alpha^*}{|f|}, \text{ PBL height} \\ G(\sigma) := \sigma(1 - \sigma)^2 \\ H \text{ Heaviside} \end{cases} \quad (2.6)$$

where  $\nu_\alpha^m$  is a background value to ensure that  $\nu_\alpha$  will remain strictly positive. In each medium, the KPP scheme predicts a parabolic profile of  $\nu_\alpha$  between the air-sea interface and the PBL (Planetary Boundary Layer) height  $h_{pbl}^\alpha$  whereas  $\nu_\alpha$  is constant outside the PBL i.e. between  $h_{pbl}^\alpha$  and  $z_\alpha^\infty$ .

### 2.3 The coupled Ekman layer problem including turbulent parametrizations

Putting all the different pieces together, we end up with the following coupled problem

$$\begin{cases} \partial_t \mathbf{u}_a - f \mathbf{k} \times (\mathbf{u}_a - \mathbf{u}_a^g) - \partial_z (\nu_a(u_a^*, f, z) \partial_z \mathbf{u}_a) = 0, & \text{in } \Omega_a \times [0, T] \\ \mathbf{u}_a(z = z_a^\infty, t) = \mathbf{u}_a^g, & \text{in } [0, T] \\ \rho_a \nu_a \partial_z \mathbf{u}_a(z = z_a^1, t) = \rho_a (u_a^*(t))^2 \mathbf{e}_\tau \end{cases} \quad (2.7)$$

$$\begin{cases} \partial_t \mathbf{u}_o - f \mathbf{k} \times (\mathbf{u}_o - \mathbf{u}_o^g) + \partial_z (\nu_o(u_o^*, f, z) \partial_z \mathbf{u}_o) = 0, & \text{in } \Omega_o \times [0, T] \\ \mathbf{u}_o(z = z_o^\infty, t) = \mathbf{u}_o^g, & \text{in } [0, T] \\ \rho_o \nu_o \partial_z \mathbf{u}_o(z = z_o^1, t) = \rho_o (u_o^*(t))^2 \mathbf{e}_\tau \end{cases} \quad (2.8)$$

where the way to evaluate  $u_\alpha^*$  is given in §2.2.1. Note that existing studies of this problem often consider simplified physics where the turbulent viscosities are held constant. Here, we aim at studying the mathematical properties of this coupled problem to assess the impact of taking into account all the complexity of the turbulent parameterizations.

## 3 SOME MATHEMATICAL RESULTS

From (2.7)-(2.8) we expect that the main difficulties in the mathematical analysis will be related to the 'mixing' term  $\partial_z (\nu_\alpha \partial_z \mathbf{u}_\alpha)$ . We, thus, focus our theoretical work on this particular term assuming stationarity and absence of rotation (i.e.  $f = 0$ ) to make an analytical study tractable.

### 3.1 Analytic determination of the coupled solution

Thanks to § 2.2.1 and § 2.2.2, we can clearly subdivide our problem into different layers reflecting different behaviors of the solution (see also Fig. 1) :

- Outside the PBL (i.e. for  $z > h_{pbl}^a$ ) the viscosity is constant meaning that the flow is not affected by the presence of the air-sea interface (this is the so-called "free atmosphere"). The solution thus behaves as

$$\partial_{zz}^2 \mathbf{u}_a = 0, \quad z \in ]h_{pbl}^a(u^*); z_a^\infty[$$

- In the PBL (i.e. for  $z_a^1 < z < h_{pbl}^a$ ) we define the KPP-A region where the solution satisfies

$$\begin{cases} \partial_z (\nu_a(u_a^*, z) \partial_z \mathbf{u}_a) &= 0, & z \in ]z_a^1, h_{pbl}^a[ \\ \nu_a \partial_z \mathbf{u}_a(z = z_a^1) &= (u_a^*)^2 \mathbf{e}_\tau \end{cases} \quad (3.1)$$

- In the surface log-layer (i.e. for  $z_a^r < z < z_a^1$ ) named LL-A region, the vertical gradients are constant and given by (the solution is thus controlled by the jump  $\llbracket \mathbf{u}_a \rrbracket_{z_a^r}^{z_a^1} = \mathbf{u}_a(z_a^1) - \mathbf{u}_a(z_a^r)$ )

$$\partial_z \mathbf{u}_a = \frac{u_a^*}{\kappa z} \mathbf{e}_\tau, \quad z \in ]z_a^r, z_a^1[$$

which is equivalent to having  $\nu_a = \kappa u_a^* z$ .

- In the viscous sublayer, referred to as VSL-A region (i.e. for  $0 < z < z_a^r$ ), we assume a linear evolution of the solution since

$$\partial_z \mathbf{u}_a = \frac{u_a^*}{\kappa z_a^r} \mathbf{e}_\tau, \quad z \in ]0, z_a^r[$$

Same applies on the oceanic side by replacing  $u_a^*$  by  $u_o^*$  as illustrated by figure 1. Note that the continuity of the momentum flux at the interface implies that  $u_o^* = \sqrt{\rho_a/\rho_o} u_a^* = \lambda u_a^*$  with  $\lambda \approx 3/100$ . The stationary solution is thus function of the value of  $u_a^*$  (which is a function of  $\mathbf{u}_s = \mathbf{u}_a(z = 0)$  and  $\mathbf{u}_1 = \mathbf{u}_a(z = z_a^1)$ ) which itself depends on the external boundary conditions ( $\mathbf{u}_\alpha^\infty = \mathbf{u}_\alpha(z = z_a^\infty)$ ). To reflect this dependency, we define the *Ekman planetary boundary function*  $\mathcal{F}_E$  as such:

$$\begin{aligned} \mathcal{F}_E : \mathbb{R}_+ &\rightarrow \mathbb{R}^2 \\ u_a^* &\mapsto \mathbf{u}_a^* - \mathbf{u}_o^\infty \end{aligned}$$

where  $u_a^*$  is directly linked to  $\mathbf{u}_1$  and  $\mathbf{u}_s$  by the following relation

$$(u_a^*)^2 = C_D \|\mathbf{u}_1 - \mathbf{u}_s\|^2 = \left( \frac{\kappa}{\ln(z_a^1/z_a^r)} \right)^2 \|\mathbf{u}_1 - \mathbf{u}_s\|^2 \quad (3.2)$$

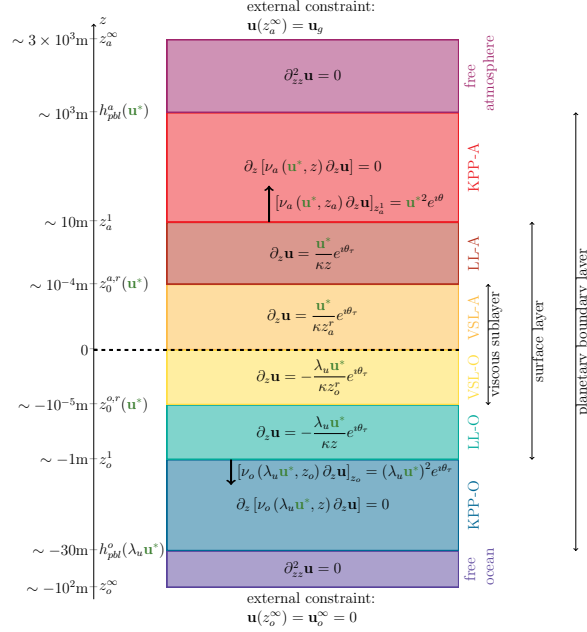


Figure 1: Sublayers for the Ekman problem, illustrating the dependencies on the  $u^*$  scale.

with  $C_D$  a drag coefficient and  $z_a^r$  is the roughness length defined in (2.5). Expression (3.2) directly arises from the application of the law of the wall (2.3)-(2.4) in the surface layer.

Since we do not consider the Coriolis term, in the remaining we decide for simplicity to align our local plane in the direction of  $\mathbf{e}_\tau$  so that we only have to consider one component of the velocity vector ( $\mathbf{u}_\alpha = (u_\alpha, 0)$ ) instead of two. Next step is to find an explicit expression for the function  $\mathcal{F}_E$ . Knowing that on each subdomain the solution satisfies  $\nu_\alpha(z, u_\alpha^*) \partial_z u_\alpha = (u_\alpha^*)^2$  we easily find that on the atmospheric side

$$\int_0^{z_a^\infty} (\partial_z u_a) dz = u_a(z_a^\infty) - u_s = (u_a^*)^2 \left\{ \int_0^{z_a^r} \frac{dz}{\kappa z_a^r u_a^*} + \int_{z_a^r}^{z_a^1} \frac{dz}{\kappa z u_a^*} + \int_{z_a^1}^{h_{\text{pbl}}^a} \frac{dz}{\nu_a(z, u_a^*)} + \int_{h_{\text{pbl}}^a}^{z_a^\infty} \frac{dz}{\nu_a^m} \right\},$$

same rationale applies on the oceanic side to determine analytically  $u_s - u_o(z_o^\infty)$ . Taking the sum of the atmospheric and oceanic solutions and explicitly computing the integrals

on the right hand side, we end up with an expression for the operator  $\mathcal{F}_E$

$$\mathcal{F}_E(u_a^*) = u_a(z_a^\infty) - u_o(z_o^\infty) = \frac{u_a^*}{\kappa} \left[ \underbrace{1 + \lambda}_{\mathcal{F}_{E,VSL}} + \underbrace{\ln\left(\frac{z_a^1}{z_a^r(u_a^*)}\right) + \lambda \ln\left(\frac{z_o^1}{-\lambda z_a^r(u_a^*)}\right)}_{\mathcal{F}_{E,LL}} \right. \\ \left. + \underbrace{\mathcal{I}_{KPP}^a(u_a^*) + \mathcal{I}_{KPP}^o(\lambda u_a^*)}_{\mathcal{F}_{E,KPP}} + \underbrace{\frac{z_a^\infty - h_{pbl}(u_a^*)}{\nu_a^m} - \frac{h_{pbl}(\lambda u_a^*) + z_o^\infty}{\nu_o^m}}_{\mathcal{F}_{E,free}} \right] \quad (3.3)$$

where the terms  $\mathcal{I}_{KPP}^\alpha$ , corresponding to the integral of the inverse of the parabolic KPP viscosity profiles are explicit and analytical functions of  $(u_a^*)$  not given here for simplicity. The different terms in the right hand side are arranged to respectively match the viscous sublayer (VSL), the surface log-layer (LL), the PBL viscosity given by the K-profile parameterization (KPP) and the free atmosphere/ocean where the viscosity corresponds to the molecular viscosity and is thus independent of the state of the air-sea interface.

Our objective is now to determine whether (3.3) is invertible, i.e. given  $\llbracket u \rrbracket_{z_o^\infty}^{z_a^\infty} = u_a(z_a^\infty) - u_o(z_o^\infty) \in \mathbb{R}_+$ , is there a scale  $u^*$  such that (3.3) is satisfied? Is this scale unique?

### 3.2 Unicity of the solution

We start by imposing a simple constraint on the value of  $z_\alpha^\infty$  to ensure that these values are larger than the planetary boundary layer thickness (i.e.  $z_a^\infty > cu_a^*/|f|$ ,  $z_o^\infty < -\lambda cu_a^*/|f|$ , with  $c$  introduced in (2.6)) which is always the case in numerical codes where the the PBL thickness is systematically limited respectively by the total depth of the ocean and the maximum height in the atmospheric model. In an equivalent way, for given values  $z_\alpha^\infty$ , this constraint is satisfied as long as the friction velocity  $u_a^*$  is bounded by  $u_m^* = \min\{z_a^\infty|f|/c, (-z_o^\infty)|f|/c\}$ . For properly chosen values of  $z_\alpha^\infty$ , Figure 2a shows the contributions from the various vertical layers to the final value of  $\mathcal{F}_E$  as a function of  $u_a^*$ . It is not surprising to see that the main contribution comes from the layer with small background viscosity since the inverse of the viscosity appears directly in the right-hand-side of (3.3). More importantly, the dashed black line in figure 2b shows that the function  $\mathcal{F}_E$  is not injective since two distinct values  $u_1^*$  and  $u_2^*$  of  $u_a^*$  can lead to the same value of  $\mathcal{F}_E$ ;  $\mathcal{F}_E(u_1^*) = \mathcal{F}_E(u_2^*) = u_a^\infty - u_o^\infty$ . This lack of invertibility is due to the contribution of the free ocean/atmosphere which is the only contribution that is not monotonically increasing with increasing  $u_a^*$  (Fig. 2b). Indeed, using the notations introduced in (3.3) we can easily show that

$$\begin{aligned} \partial_{u_a^*} \mathcal{F}_{E,VSL} &= 2/\kappa > 0, & \forall u_a^* \in \mathbb{R}_+ \\ \partial_{u_a^*} \mathcal{F}_{E,LL} &> 0 & \forall u_a^* \in ]0; u_{\max}^*[, u_{\max}^* \approx 30 \text{ m s}^{-1} \\ \partial_{u_a^*} \mathcal{F}_{E,KPP} &> 0 & \forall u_a^* \in \mathbb{R}_+ \end{aligned} \quad (3.4)$$

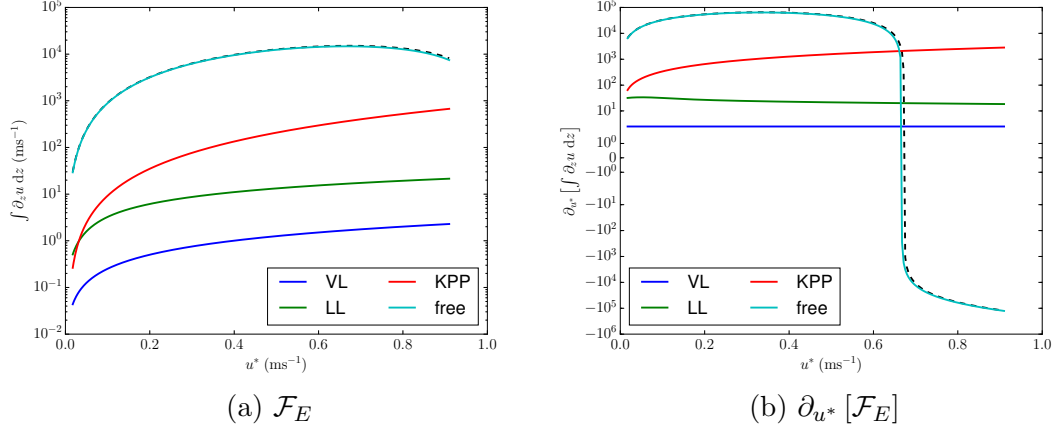


Figure 2: Different contributions in the  $\mathcal{F}_E$  operator (a) and  $\partial_{u^*} [\mathcal{F}_E]$  (b), using the subdivision described in (3.3). Here, the maximum value for  $\llbracket u \rrbracket_0^{z_a^1}$  is  $20 \text{ m s}^{-1}$ , leading to  $u_m^* \sim 0.7 \text{ ms}^{-1}$ , through equation (3.2). The colored lines represent the different contributions from all four types of sublayers; the dashed black line being their sum, which are respectively  $|u_a^\infty|$  and  $\partial_{u^*}|u_a^\infty|$ . Here,  $z_a^1 = 10 \text{ m}$ ,  $z_o^1 = -3 \text{ m}$ ,  $\nu_m^1 = 10^{-4} \text{ m}^2 \text{ s}^{-1}$ ,  $\nu_m^a = \nu_m^1 / \lambda^2$ ,  $z_a^\infty = 1.1 \times h_{pbl}(u_a^*(\llbracket u \rrbracket_0^{z_a^1} = 20 \text{ m s}^{-1}))$  and  $z_o^\infty = -\lambda z_a^\infty$ .

which means that  $\forall u_a^* \leq u_{\max}^*$  we will systematically get that  $\partial_{u^*} \mathcal{F}_E \geq \partial_{u^*} \mathcal{F}_{E,\text{free}}$ . Note that the value of  $u_{\max}^*$  is unrealistically large, such large values of  $u_a^*$  are not expected to occur in realistic simulations even in the case of extreme events like tropical cyclones meaning that the special case  $u_a^* \geq u_{\max}^*$  does not have to be considered here. If we now note  $u_b^*$  (resp.  $u_{b,\text{free}}^*$ ) the only nonzero root of  $\partial_{u_a^*} \mathcal{F}_E$  (resp.  $\partial_{u_a^*} \mathcal{F}_{E,\text{free}}$ ) we get from (3.4) that  $u_b^* \geq u_{b,\text{free}}^*$ . Moreover, we can analytically find

$$u_{b,\text{free}}^* = \frac{2|f|}{3c} \left[ \frac{z_a^\infty}{\nu_m^a} - \lambda^2 \frac{z_o^\infty}{\nu_m^o} \right]. \quad (3.5)$$

As a consequence, as long as  $u^*$  stays within the bounds  $]0, u_{b,\text{free}}^*]$  invertibility of the function  $\mathcal{F}_E$  is guaranteed and the solution of the associated coupled problem is unique. The strategy is then to choose  $(z_a^\infty, z_o^\infty)$  so that  $u_a^*$  is guaranteed to be in  $]0, u_{b,\text{free}}^*]$ . We introduce in the following section a coupling algorithm specifically built to enforce this constraint.

#### 4 THE COUPLING ALGORITHM

This section will first describe the algorithm used for the coupling of the Ekman layers, before presenting numerical results. The objective of this algorithm is to properly select the altitude  $z_a^\infty$  and the depth  $z_o^\infty$  at which the external data are provided to ensure a physically sound solution. In practice  $z_a^\infty$  and  $z_o^\infty$  can indeed be considered as degrees



of freedom as soon as they are located outside the boundary layers i.e. far from the influence of the interface. Once  $z_a^\infty$  and  $z_o^\infty$  are chosen we can then extract the boundary conditions  $u_a(z_a^\infty)$  and  $u_o(z_o^\infty)$  from a three-dimensional simulation before starting the coupling process for the planetary boundary layers. With this methodology we avoid coupling the entire atmospheric and oceanic model by only modifying the region of the solution that it is influenced by the coupling and leaving unchanged the solution in the free ocean and free atmosphere. This approach is expected to enable a substantial gain in efficiency while ensuring unicity of the solution.

#### 4.1 Description

The objective of the algorithm is basically to invert the  $\mathcal{F}_E$  operator, as described in (3.3), avoiding convergence toward a non-physically acceptable solution. We suggest here simple fixed point iterations.

Initialization step :

1. Select a maximum allowed value  $u_{\max}^*$  such that the expected solution  $u_a^* \in [0, u_{\max}^*]$ .
2. From  $u_{\max}^*$ , compute  $z_a^\infty$  and  $z_o^\infty$  to ensure unicity of the solution. Using (3.5), the idea is to choose  $z_a^\infty$  and  $z_o^\infty$  such that  $u_{\max}^* = u_{b,\text{free}}^*$  and  $z_o^\infty = -\lambda z_a^\infty$ .
3. Select the values  $u_a(z_a^\infty)$  et  $u_o(z_o^\infty)$  for the external boundary conditions.

Fixed point iterations :

The purpose is to create a sequence  $(u_k^*)_{k \in \mathbb{N}}$  such that  $u_k^* \rightarrow u_{\text{sol}}^*$ , with  $u_{\text{sol}}^*$  the unique fixed point, only using  $u_a^\infty$  and  $u_o^\infty$  as inputs.  $u_{k=0}^*$  can be taken arbitrarily as long as  $u_{k=0}^* \leq u_{\max}^*$  is satisfied. Then, an iterative loop begins

- (i) From the  $u_k^*$  scale, compute all the integrals in the  $\mathcal{F}_E$  function (3.3). Also compute its gradient with regard to  $u_k^*$ ,  $\partial_{u^*} [\mathcal{F}_E]_{u_k^*}$ . Compute  $z_{a,k}^r$  from  $u_k^*$  via (2.5) and  $z_{o,k}^r = -\lambda z_{a,k}^r$ .

- (ii) Compute

$$\llbracket u \rrbracket_{0,k}^{z_a^1} = \llbracket u \rrbracket_{z_o^\infty}^{z_a^\infty} - \mathcal{F}_E(u_k^*) + \frac{u_k^*}{\kappa} \left[ 1 + \ln \left( \frac{z_a^1}{z_{a,k}^r} \right) \right] \quad (4.1)$$

- (iii) Assess

$$C_{D,k} = \left( \frac{\kappa}{\ln(z_a^1/z_{a,k}^r)} \right)^2 \quad (4.2)$$

- (iv) Convergence is supposed to be reached when (4.1) and (4.2) satisfy:

$$u_k^{*2} \approx C_{D,k} \times \left| \llbracket u \rrbracket_{0,k}^{z_a^1} \right|^2 \quad (4.3)$$

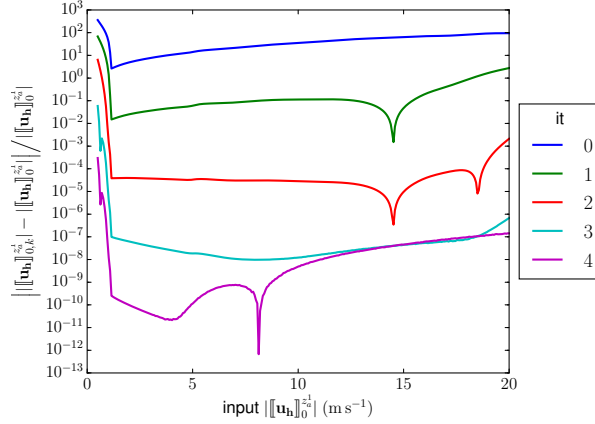


Figure 3: Results obtained with the algorithm described in Section 4.1. This figure shows the relative error between the input  $||u||_0^{z_a^1}$  and the iterated values  $||u||_{0,k}^{z_a^1}$ , computed through (4.1). Each line represents a different iteration. Here,  $z_o^1 = -3$  m,  $z_a^1 = 10$  m.

up to an arbitrary numerical precision. If (4.3) is not satisfied, then go back to (i) with

$$u_{k+1}^* = u_k^* + \frac{||u||_{0,k}^{z_a^1} - u_k^* / \sqrt{C_{D,k}}}{\partial_{u^*} [\mathcal{F}_E^0]_{u_k^*}} \quad (4.4)$$

## 4.2 Numerical results

Figure 3 illustrates that following the procedure described above, convergence toward a physically acceptable solution is obtained in a few iterations. Generally speaking a fast convergence is expected for air-sea coupling problems because of the large jump in densities between the ocean and the atmosphere. Indeed one component (the atmosphere) is very fast and adjusts itself quickly to the slow component (the ocean).

## 5 CONCLUSION AND PERSPECTIVES

In this paper we have introduced a coupled Ekman layer problem, emphasizing the influence of the underlying turbulent parameterizations and closure assumptions on the unicity of the solutions. Thanks to a thorough mathematical analysis of the coupled problem we have been able to propose a simple procedure which guarantees that a unique physically sound solution is obtained. The work presented here should be interpreted as a first step toward building satisfactory coupling algorithms for Ekman layers (and possibly stratified Ekman layers). Using the formalism introduced here, our objective is to progressively discard restrictive hypotheses, namely:

1. Incorporating effects due of the Coriolis force. This would change the mathematical structure of the problem, as the solution profiles in the KPP-layers could not simply

be expressed thanks to an invariant gradient, as in (3.1). Incorporating Coriolis effects would mean solving a Sturm-Liouville problem with complex coefficients, for which there are mathematical results of existence and unicity [9]; however, obtaining analytical results at a continuous level is expected to become much more tedious.

2. Taking fluid stratification into account, ie. considering a non-constant temperature  $T$  as a prognostic variable. A consequence is that the parameterizations of the boundary layers and of air-sea fluxes will become much more complicated to analyze since they greatly depend on the stability of the air/water column (i.e. if the temperature is decreasing or increasing with altitude/depth).
3. Further investigating the impact of the viscous sublayer parameterization. State of art surface layer parameterizations typically assume that given the thinness of viscous sublayers,  $\mathbf{u}_\alpha$  can be considered as constant in this region. While this is numerically accurate, we believe that including the viscous layer influence in the air-sea flux parameterizations should systematically be done within the log-layer, for ensuring the self-consistency of the coupling problem at a continuous level. Indeed, not including the viscous sublayer leads to a friction velocity of the form (3.2), i.e.  $u_a^{*2} = C_D \times \left\| \llbracket \mathbf{u}_a \rrbracket_{z_a^r}^{z_a^1} \right\|$ , while, following pioneering mathematical results [10], the jump in wind speed should be taken from  $z = 0$  and not from  $z = z_a^r$ . The drag coefficient  $C_D$  in (3.2) can be rewritten as:

$$\frac{\kappa}{\sqrt{C_D}} = \ln(z_a^1/z_a^r) + \gamma_{VL} \quad (5.1)$$

where  $\gamma_{VL}$  should incorporate viscous layer parameterization effects. Our choice of assuming constant vertical gradient in the viscous layer leads to  $\gamma_{VL} = 1$ .

4. Study the time-dependent problem, ie. reintroduce the  $\partial_t u$  term to the equations of the Ekman layer problem.

## Acknowledgements

The authors acknowledge the support of the French national research agency (ANR) through contract ANR-16-CE01-0007.

## REFERENCES

- [1] F. Lemarié, E. Blayo, and L. Debreu. Analysis of ocean-atmosphere coupling algorithms: Consistency and stability. *Procedia Computer Science*, 51(0):2066 – 2075, 2015.
- [2] A. Beljaars, E. Dutra, G. Balsamo, and F. Lemarié. On the numerical stability of surface-atmosphere coupling in weather and climate models. *Geoscientific Model Development*, 10(2):977–989, 2017.

- [3] C. Pelletier, F. Lemarié, and E. Blayo. Sensitivity analysis and metamodels for the bulk parameterization of turbulent air-sea fluxes. *Q. J. R. Meteorol. Soc.*, 2017. submitted.
- [4] D.M. Lewis and S.E. Belcher. Time-dependent, coupled, Ekman boundary layer solutions incorporating Stokes drift. *Dynamics of Atmospheres and Oceans*, 37(4):313–351, 2004.
- [5] J.A. Bye. Inertially coupled Ekman layers. *Dynamics of atmospheres and oceans*, 35(1):27–39, 2002.
- [6] W. G. Large, J. C. McWilliams, and S. C. Doney. Oceanic vertical mixing: A review and a model with a nonlocal boundary layer parameterization. *Reviews of geophysics*, 32(4):363–403, 1994.
- [7] J. C. McWilliams and E. Huckle. Ekman layer rectification. *Journal of Physical Oceanography*, 36:1646–1659, 2005.
- [8] S. D. Smith. Coefficients for sea surface wind stress, heat flux, and wind profiles as a function of wind speed and temperature. *Journal Of Geophysical Research*, 93(C12):15467–15472, 1988.
- [9] B. M. Brown, D. K. R. McCormack, W. D. Evans, and M. Plum. On the spectrum of second-order differential operators with complex coefficients. *Proceedings of the Royal Society of London A: Mathematical, Physical and Engineering Sciences*, 455(1984):1235–1257, 1999.
- [10] J.L. Lions, R. Temam, and S. Wang. Mathematical theory for the coupled atmosphere-ocean models (CAO III). *Journal de Mathématiques Pures et Appliquées*, 74:105–163, 1995.